Exploration of Targeted Anti-tumor Therapy

Open Exploration

Open Access Original Article

Macrophage-like phenotypes of tumor-immune hybrid cells in primary breast cancer

Evgeniya S. Grigoryeva*, Elena O. Shmakova, Elena V. Koylova, Anna Yu. Kalinchuk, Liubov A. Tashireva

The Laboratory of Molecular Therapy of Cancer, Cancer Research Institute, Tomsk National Research Medical Center, Russian Academy of Sciences, Tomsk 634009, Russia

***Correspondence:** Evgeniya S. Grigoryeva, The Laboratory of Molecular Therapy of Cancer, Cancer Research Institute, Tomsk National Research Medical Center, Russian Academy of Sciences, Tomsk 634009, Russia. grigoryeva.es@gmail.com
Academic Editor: Francesk Mulita, General Hospital of Aigio, Greece
Received: March 30, 2026 **Accepted:** August 25, 2026 **Published:** November 9, 2026

Cite this article: Grigoryeva ES, Shmakova EO, Koylova EV, Kalinchuk AY, Tashireva LA. Macrophage-like phenotypes of tumor-immune hybrid cells in primary breast cancer. Explor Target Antitumor Ther. 2026;7:1002411. https://doi.org/10.37349/etat.2026.1002411

Abstract

Aim: Tumor-immune hybrid cells (THCs) co-expressing leukocyte and epithelial markers arise from cell fusion and may contribute to cancer progression. However, the phenotypic heterogeneity of THCs, their association with macrophage lineage markers, and their clinical significance in breast cancer (BC) remain poorly characterized.

Methods: Using multicolor flow cytometry, we analyzed primary breast tumors from 42 patients to characterize THCs expressing pan-leukocyte antigen cluster of differentiation 45 (CD45) together with epithelial markers epithelial cell adhesion molecule (EpCAM) and/or pan-cytokeratin. Expression of macrophage/monocyte-associated markers (CD68, CD163, CD16, CD206) was assessed across THC subpopulations.

Results: THCs were heterogeneous, with $CD45^+EpCAM^+panCK^-$ and $CD45^+EpCAM^+panCK^+$ subpopulations being most frequent, whereas $CD45^+EpCAM^-panCK^+$ hybrids were rare. Within $EpCAM^+$ THCs, a substantial proportion expressed M2-like markers ($CD163^+$, $CD206^+$), indicating an immunosuppressive, pro-tumor phenotype. The proportion of THCs carrying macrophage markers was increased in larger tumors (T2) and in node-positive cases (N1–3). Patients with the luminal B [human epidermal growth factor receptor 2 $(HER2)^-$] subtype—characterized by higher proliferative activity—showed a significant enrichment of hybrids expressing CD163 and CD206. Notably, specific rare THC subpopulations were associated with distant metastasis during follow-up: the $CD68^+CD163^+CD16^-CD206^-$ phenotype within the $CD45^+EpCAM^-panCK^+$ fraction and the $CD68^-CD163^-CD16^-CD206^+$ phenotype within the $CD45^+EpCAM^+panCK^+$ fraction. The former, despite its very low frequency (cutoff 0.65%), showed the highest diagnostic accuracy (95.65%) for predicting poorer survival ($p = 0.012$).

Conclusions: The predominance of M2-like THCs in more aggressive breast tumors, along with the identification of rare hybrid phenotypes associated with distant metastasis, underscores the clinical significance of these cells. Validation in larger cohorts is warranted to establish their utility as prognostic biomarkers and to elucidate their functional role in BC progression.

© The Author(s) 2026. This is an Open Access article licensed under a Creative Commons Attribution 4.0 International License (https://creativecommons.org/licenses/by/4.0/), which permits unrestricted use, sharing, adaptation, distribution and reproduction in any medium or format, for any purpose, even commercially, as long as you give appropriate credit to the original author(s) and the source, provide a link to the Creative Commons license, and indicate if changes were made.

Keywords

tumor microenvironment, tumor-immune hybrid cells, tumor heterogeneity, breast cancer, prognosis

Introduction

As a heterogeneous disease, breast cancer (BC) prognosis and treatment depend on the tumor's intrinsic biological features. The standard predictive and prognostic BC biomarkers include estrogen/progesterone receptor expression, human epidermal growth factor receptor 2 (HER2) expression, and Ki-67 proliferative index [1]. However, substantial variability in disease outcomes within each molecular subtype underscores the need to develop and validate additional prognostic markers capable of assessing individual patient prognosis.

The tumor microenvironment (TME) is a complex ecosystem where cancer cells continuously interact with a variety of stromal and immune cells, fundamentally shaping disease progression and therapeutic response [2]. Among these interactions, the fusion of cancer cells with immune cells has emerged as a mechanism capable of generating tumor-immune hybrid cells (THCs) [3, 4]. These hybrid cells often acquire a unique amalgamation of traits from both parental cell types, including the migratory and invasive properties of immune cells combined with the proliferative capacity of cancer cells, thereby potentially facilitating metastasis and immune evasion [5]. The formation of THCs can occur through multiple mechanisms, including direct cell fusion, trogocytosis (absorbs membrane components), and aberrant expression of lineage-specific markers [6].

Accumulating evidence suggests that macrophages are a significant component of the TME and are frequently implicated in the formation of THCs [7]. Tumor-associated macrophages (TAMs) can exhibit distinct polarization states, with M2-macrophages generally promoting immunosuppression, angiogenesis, and tumor progression [8]. Notably, experimental studies have indicated that M2-polarized monocytes may possess a higher capacity to fuse with cancer cells compared to M1, giving rise to highly invasive hybrid cells [9]. However, the precise composition, phenotypic heterogeneity, and clinical relevance of these hybrid populations within primary human tumors remain poorly defined. Moreover, macrophage functional classification has evolved beyond the traditional M1-M2 paradigm [10], yet a detailed analysis of THCs within this expanded framework remains lacking.

Previous studies have confirmed the existence of THCs expressing both leukocyte [e.g., cluster of differentiation 45 (CD45)] and epithelial [e.g., epithelial cell adhesion molecule (EpCAM), cytokeratins] markers [11, 12] and have demonstrated their pronounced clinical significance in tumor progression across several tumor types. According to Akhter et al. [11], the $EpCAM^+CD45^+$ population is highly invasive, shows a mesenchymal gene expression pattern, and contains $CD133^+$ and $CD117^+CD44^+$ stem cell subpopulations. Authors reveal that these cells evade natural killer (NK) cell-mediated immune surveillance through overexpression of major histocompatibility complex class I antigens. However, the prevailing data have been obtained from circulation or ascitic fluid, leaving the site of hybrid cell origin unclear. Thus, a comprehensive characterization of hybrid cells phenotypic variants in primary tumor, especially in the context of their association with specific immune cell lineages and their clinical implications, is still lacking. The heterogeneity of THCs, their relationship with macrophage polarization markers (such as CD68, CD163, CD206), and their potential correlation with aggressive clinicopathological features, molecular subtypes, and patient prognosis warrant further investigation.

The use of multicolor flow cytometry enables detailed analysis of the phenotypic heterogeneity of hybrid cells within tumor tissue, allowing comprehensive assessment of diverse expression patterns of epithelial and immune markers [13]. In this study, we aimed to characterize the phenotypic heterogeneity of THCs co-expressing the pan-leukocyte marker CD45 and epithelial markers EpCAM and/or pan-cytokeratin in primary breast tumors. Our objectives were to define distinct hybrid subpopulations, assess their expression of macrophage/monocyte lineage markers, and evaluate their associations with key clinicopathological features, molecular subtypes, and disease prognosis. By identifying specific hybrid

phenotypes linked to tumor aggressiveness and distant metastasis, this work seeks to advance understanding of the role of cell fusion in BC progression and to uncover potential novel prognostic markers.

Materials and methods

Patients

The prospective observational study enrolled 42 patients diagnosed with BC ranging from stage T1-4N0-3M0, who were admitted for treatment at the Cancer Research Institute, Tomsk NRMC (Table 1). The study received approval from the local ethics committee of the Tomsk NRMC Institutional Review Board on August 25, 2020, with approval No. 7, and was conducted in accordance with the Declaration of Helsinki (1964, with amendments from 1975 and 1983). All patients granted informed consent before participating in the analysis. Patients were treated according to ESMO Clinical Practice Guidelines [14]. The follow-up period was 3 years.

Table 1. Clinicopathological characteristics of breast cancer patients.

Parameter		Frequency, % (*n*)
Age	< 35	2.38% (1/42)
	35–50	33.33% (14/42)
	> 50	64.29% (27/42)
Tumor size	T1	54.76% (23/42)
	T2	40.48% (17/42)
	T3	0.00% (0/42)
	T4	4.76% (2/42)
Tumor grade	I	26.19% (11/42)
	II	66.67% (28/42)
	III	7.14% (3/42)
Molecular subtype	Luminal A	66.67% (28/42)
	Luminal B ($HER2^-$)	16.67% (7/42)
	Luminal B ($HER2^+$)	7.14% (3/42)
	Triple-negative	4.76% (2/42)
	$HER2^+$	4.76% (2/42)
Lymphovascular invasion	Yes	23.81% (10/42)
	No	76.19% (32/42)
Distant metastasis	Yes	9.52% (4/42)
	No	90.48% (38/42)
Lymph node metastasis	Yes	30.95% (13/42)
	No	69.05% (29/42)

Flow cytometry

Fresh frozen cancer tissue samples were mechanically disaggregated using the BD Medimachine System (BD Biosciences, USA) for cell suspensions. Initially, 500 µL of the OptiLyse C buffer (Beckman Coulter; France) was added to the samples for erythrocyte lysis, then the samples were washed in 2 mL of the CellWASH solution (BD Biosciences; USA) for 10 min at 300 *g*, with subsequent removal of supernatant. The staining procedure consisted of 2 steps: surface and intracellular staining preceded by cell permeabilization. In the first step, 5 µL of the BV570 anti-human CD45 (clone HI30, Sony Biotechnology, USA), BV605 anti-human CD326 (EpCAM) (clone 9C4, Sony Biotechnology, USA), APC-Cy7 anti-human CD68 (clone Y1/82A, Sony Biotechnology, USA), BV510 anti-human CD16 (clone B73.1, Biolegend, USA), BV785 anti-human CD206 (clone 5-2, Sony Biotechnology, USA), PE-Cy7 anti-human CD163 (clone GHI/63, Sony Biotechnology, USA), PE-VISTA (clone A17207I, Biolegend, USA), Trem1-APC (clone TR3MBL1, Thermo Fischer Scientific, USA), IL10-efluor 450 (clone JES3-9D7, Thermo Fischer Scientific, USA), IL12-PerCP-efluor710 (clone MQ1-17H12, eBioscience, USA) monoclonal antibodies were added to the primary

tumor cell suspension and incubated in the dark at room temperature for 20 min. During the intracellular staining step, each stained sample was supplemented with 250 µL of the BD Cytofix/Cytoperm solution (BD Biosciences; USA), incubated in the dark for 30 min at 4°C, and then twice washed in 1 mL of the BD Perm/Wash buffer (BD Biosciences; USA) when centrifuged at 300 *g* for 6 min. A total of 50 µL of the Cell Staining Buffer (Sony Biotechnology; USA) was added to the samples; the stained samples were supplemented with 5 µL of the AF488-anti-human pan-cytokeratin antibody (clone AE1/AE3; Thermo Fischer Scientific, USA) and incubated at 4°C for 20 min. After that, each sample was washed in 1 mL of the CellWASH buffer (BD Biosciences; USA) by centrifugation at 300 *g* for 6 min. In the final phase, 100 µL of the Cell Staining Buffer (Sony Biotechnology; USA) was added to precipitate, and the sample was resuspended.

Both unstained control and antibody quality control assessments were performed. The appropriate isotype antibodies were added to the isotype control sample at equivalent concentrations. Compensation beads (VersaComp Antibody Capture Bead kit, Beckman Coulter, Indianapolis, IL, USA) were utilized for compensation control. Flow cytometry analysis was conducted using the Novocyte 3000 (ACEA Biosciences, San Diego, CA, USA). The gating strategy was as follows: debris, dead cells, and doublets were initially discriminated using forward (FSC) and side scatter (SSC) parameters, and subsequent analysis was performed on $CD45^-$ cells (tumor cells) and $CD45^+$ cells (THCs). The expression of epithelial markers (EpCAM and pan-cytokeratin) and macrophage/monocyte markers (CD68, CD16, CD163 and CD206) was evaluated (Figure S1). The BC cell line MCF-7 served as a positive control for epithelial markers (EpCAM and pan-cytokeratin) staining and as a negative control for CD45 staining, whereas U937 cells were used as a positive control for CD45 staining and as a negative control for EpCAM and pan-cytokeratin staining.

Statistical analysis

The data distribution was evaluated and found to be non-normal. Therefore, non-parametric statistical methods were employed for the analysis. The data were analyzed using GraphPad Prism 9 (GraphPad Software, San Diego, CA, USA). The Mann-Whitney test was used for comparisons between two independent groups, and the Kruskal-Wallis test was applied for comparisons involving three or more independent groups. For dependent variables, the Wilcoxon test and Dunn's multiple comparisons test were used. Receiver operating characteristic (ROC) curve analysis was performed to determine the optimal cutoff and evaluate the prognostic value of the studied parameters. A *p*-value of less than 0.05 was considered statistically significant.

Results

Characterization of THCs in the primary tumor of patients with BC

THCs in primary breast tumors were identified as cells expressing the pan-leukocyte marker CD45 and at least one of the epithelial markers studied (EpCAM and/or pan-cytokeratin). Given that THCs are tumor cell derivatives, we estimated the proportion of hybrids within the total tumor cell pool. The median proportion of THCs among tumor cells was 9.9% (2.5–23.15%). However, in both cases, the absolute number of THCs exceeded the number of conventional tumor cells by 2.6- and 1.5-fold, respectively.

The frequency of $CD45^+EpCAM^+panCK^-$, $CD45^+EpCAM^+panCK^+$, and $CD45^+EpCAM^-panCK^+$ cells was 95.24% (40/42), 88.10% (37/42), and 69.05% (29/42), respectively. Moreover, $CD45^+EpCAM^-panCK^+$ cells were significantly less common compared to $CD45^+EpCAM^+panCK^-$ cells ($p = 0.0033$) and showed a trend toward being less frequent than $CD45^+EpCAM^+panCK^+$ cells ($p = 0.06$). Evaluation of the subpopulation composition showed that the proportion of THCs with mono-expression of the epithelial marker pan-cytokeratin was the lowest ($p = 0.0042$ and $p < 0.0001$) (Figure 1).

It is noteworthy that the least rare $EpCAM^-panCK^+$ cells among hybrids were predominant among tumor cells, identified as the $CD45^-$ subpopulation expressing EpCAM and/or pan-cytokeratin (Figure 2). The median proportions of $EpCAM^-panCK^+$, $EpCAM^+panCK^-$, and $EpCAM^+panCK^+$ cells were 66.30% (45.29–95.38%), 16.67% (1.47–29.13%), and 5.21% (0.86–11.78%), respectively. The frequencies of these

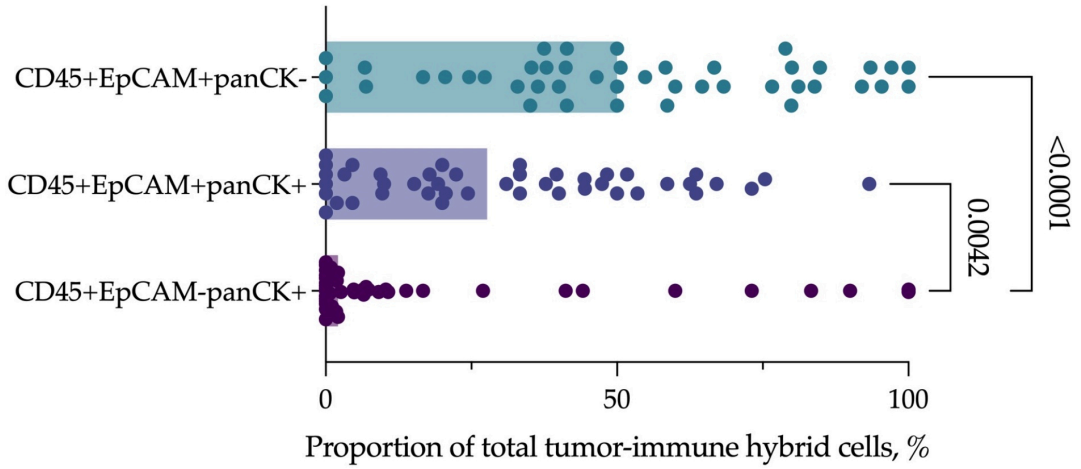


Figure 1. The proportion of tumor-immune hybrid cell subpopulations in primary tumor of breast cancer, *n* = 42.

populations did not differ significantly and were 100% (43/43), 90.70% (39/43), and 90.70% (39/43), respectively. This suggests that the $CD45^-EpCAM^-panCK^+$ cells have a low potential for hybridization with $CD45^+$ cells. In other words, the absence of EpCAM expression likely limits the ability of tumor cells to fuse with leukocyte-origin cells within the primary tumor.

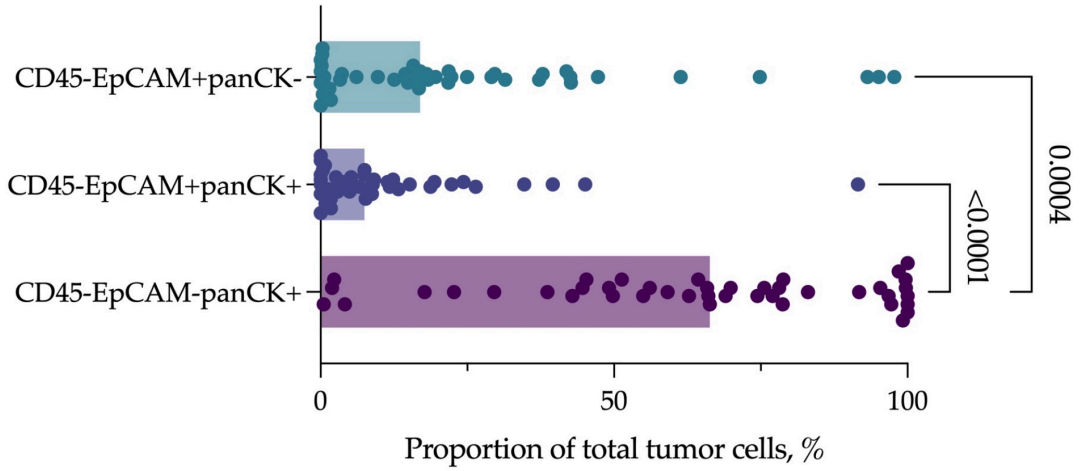


Figure 2. The proportion of tumor cell subpopulations in the primary tumor of breast cancer, *n* = 42.

Taking into account that macrophages constitute a significant part of the TME [15, 16], we assessed the expression of macrophage/monocyte markers CD68 and CD16, as well as functional polarization markers CD163 and CD206, in individual subpopulations of hybrid cells (Figures 3, 4 and 5). Among the $CD45^+EpCAM^+panCK^-$ hybrid cells, four subpopulations showed the highest proportions, including cells lacking expression of the studied markers ($CD68^-CD163^-CD16^-CD206^-$) and three subpopulations characterized by expression of the M2 macrophage marker CD206. In two of these subpopulations, co-expression of the M1 polarization marker CD163 was also observed ($CD68^+CD163^+CD16^-CD206^+$ and $CD68^-CD163^+CD16^-CD206^+$) (Figure 3). The median proportions of $CD68^-CD163^-CD16^-CD206^-$, $CD68^+CD163^+CD16^-CD206^+$, $CD68^-CD163^+CD16^-CD206^+$, and $CD68^-CD163^-CD16^-CD206^+$ cells were 8.40% (0.00–24.35%), 24.35% (1.50–36.70%), 21.00% (11.08–42.90%), and 8.55% (0.45–25.00%), respectively.

Among the $CD45^+EpCAM^+panCK^+$ hybrid cells, the predominant population lacked expression of the studied markers ($CD68^-CD163^-CD16^-CD206^-$), with a median proportion of 45.00% (18.95–79.40%) (Figure 4). A notable proportion consisted of cells co-expressing CD163 and CD206 ($CD68^-CD163^+CD16^-CD206^+$), with a median of 6.70% (0.00–31.50%), as well as the $CD68^+CD163^+CD16^-CD206^+$ cells, with a median of 0.75% (0.00–14.15%).

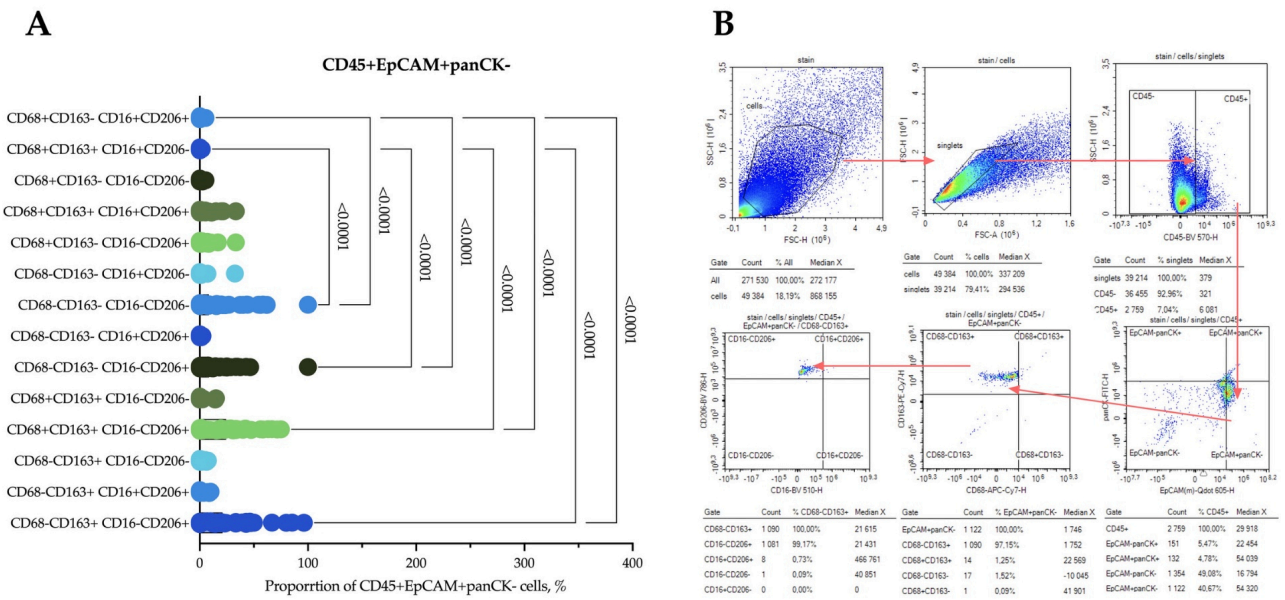


Figure 3. Flow cytometry analysis of tumor tissue from a patient with breast cancer. (**A**) The expression of macrophage/monocyte markers CD68, CD163, CD16 and CD206 in CD45$^+$EpCAM$^+$panCK$^-$ tumor-immune hybrid cells, *n* = 42. (**B**) Analysis of flow cytometry data using the CD45$^+$EpCAM$^+$panCK$^-$ cell population as a representative example. panCK: pan-cytokeratin.

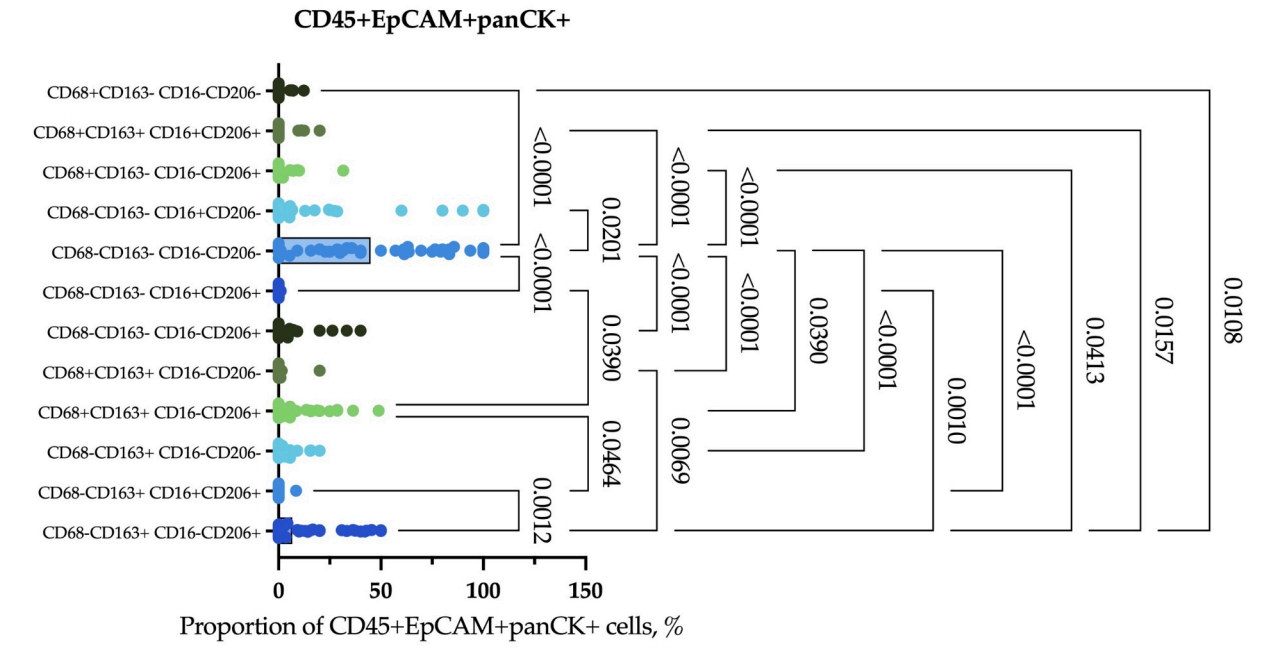


Figure 4. The expression of macrophage/monocyte markers CD68, CD163, CD16 and CD206 in CD45$^+$EpCAM$^+$panCK$^+$ tumor-immune hybrid cells, *n* = 42.

The CD45$^+$EpCAM$^-$panCK$^+$ hybrid cell population was predominantly composed of cells lacking expression of the studied macrophage/monocyte markers (CD68$^-$CD163$^-$CD16$^-$CD206$^-$), and the median proportion was 50.0% (3.58–100.0%) (Figure 5).

Thus, cells with monoexpression of pan-cytokeratin (CD45$^+$EpCAM$^-$panCK$^+$), which represent the smallest fraction of the hybrid cell population, are characterized by the highest proportion of cells lacking expression of the macrophage/monocyte markers CD68, CD163, CD16, and CD206 (Figure 6). In contrast, cells comprising the major clusters of hybrid cells (CD45$^+$EpCAM$^+$panCK$^-$ and CD45$^+$EpCAM$^+$panCK$^+$) are predominantly characterized by expression of CD163 and CD206, regardless of CD68 expression.

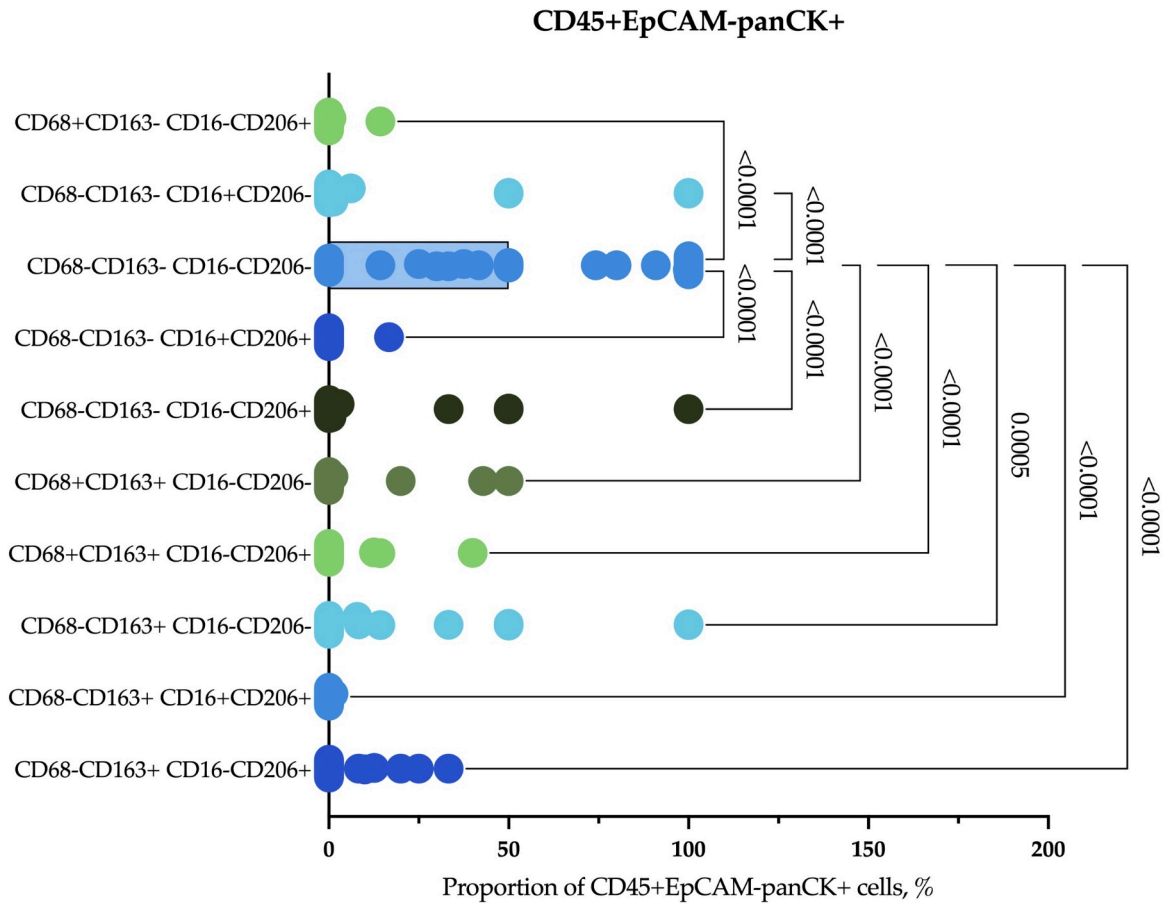


Figure 5. The expression of macrophage/monocyte markers CD68, CD163, CD16 and CD206 in CD45$^+$EpCAM$^-$panCK$^+$ tumor-immune hybrid cells, *n* = 42.

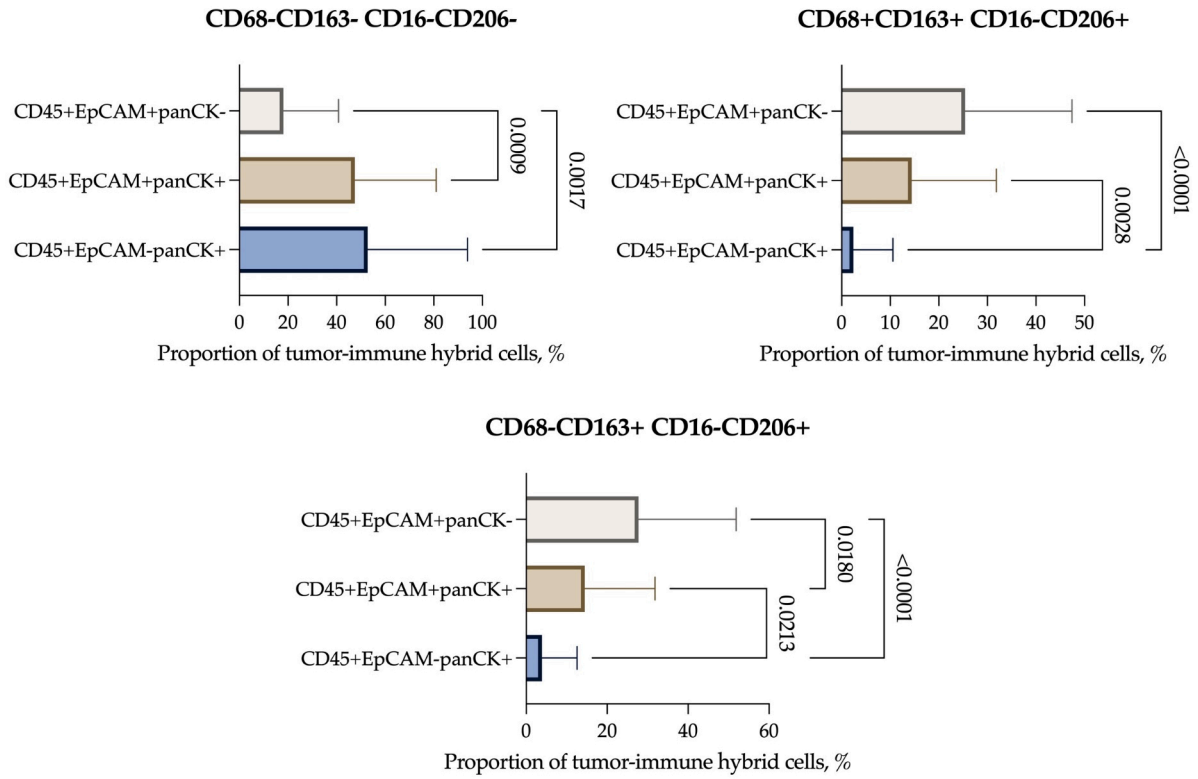


Figure 6. Comparison of macrophage/monocyte marker-expressing subpopulations among CD45$^+$EpCAM$^+$panCK$^-$, CD45$^+$EpCAM$^+$panCK$^+$, and CD45$^+$EpCAM$^-$panCK$^+$ tumor-immune hybrid cells, *n* = 42.

Association of THCs in the primary tumor with clinicopathological characteristics of BC

A study was conducted to investigate the relationship between the subpopulation composition of hybrid cells and clinicopathological parameters in BC patients. Assessment of the proportions of hybrid cells with various expression patterns of macrophage/monocyte markers CD68, CD163, CD16, and CD206 in patients stratified by the T parameter revealed some associations (Figure 7).

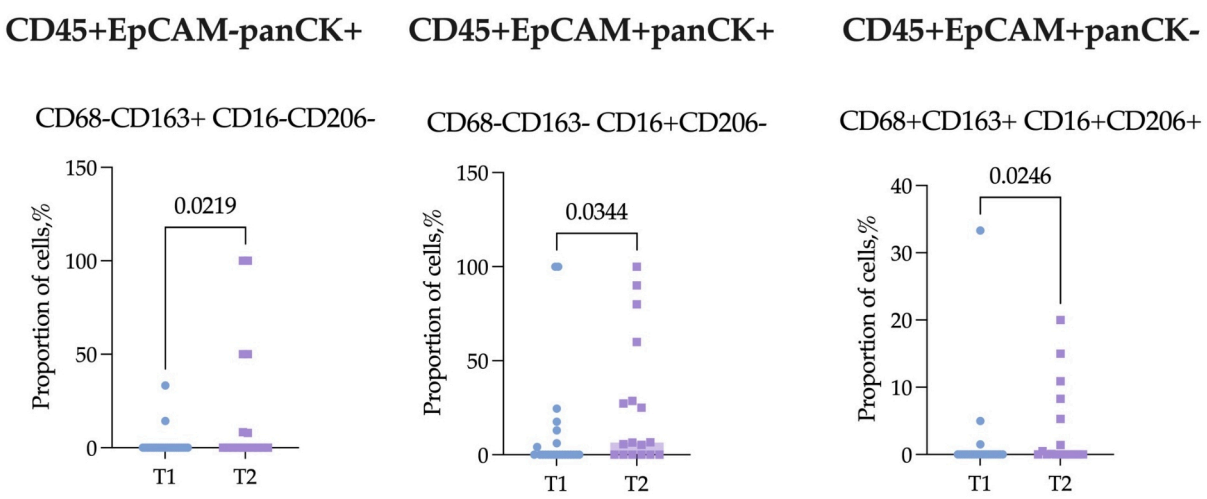


Figure 7. Expression patterns of macrophage/monocyte markers CD68, CD163, CD16, and CD206 in patients stratified by the T parameter, *n* = 42.

Patients with T2 tumor size exhibited an increased proportion of marker-expressing cells within the $CD45^+EpCAM^-panCK^+$, $CD45^+EpCAM^+panCK^+$, and $CD45^+EpCAM^+panCK^-$ subpopulations (Figure 7). Specifically, in the $CD45^+EpCAM^-panCK^+$ hybrid subpopulation, an increase was observed in the proportion of $CD68^-CD163^+CD16^-CD206^-$ cells; the median proportions in patients with T1 and T2 tumors were 0.00% (0.00–0.00%) and 0.00% (0.00–39.58%), respectively ($p = 0.0219$). Among the $CD45^+EpCAM^+panCK^+$ and $CD45^+EpCAM^+panCK^-$ hybrid cell subpopulations, an increase in the proportions of $CD68^-CD163^-CD16^+CD206^-$ and $CD68^+CD163^+CD16^+CD206^+$ cells, respectively, was also observed. The median proportion of $CD68^-CD163^-CD16^+CD206^-$ cells in patients with T1 and T2 tumors was 0.00% (0.00–6.20%) and 6.50% (0.00–44.30%), respectively ($p = 0.0344$). The median proportion of $CD68^+CD163^+CD16^+CD206^+$ cells in patients with T1 and T2 tumors was 0.00% (0.00–6.20%) and 0.00% (0.00–6.80%), respectively ($p = 0.0246$).

An assessment of the relationship between various hybrid cell subpopulations and lymph node involvement showed that patients with N1–3 stage disease exhibited a higher proportion of CD16-positive $CD45^+EpCAM^+panCK^+$ cells ($CD68^-CD163^-CD16^+CD206^-$) compared to N0 patients ($p = 0.0323$) (Figure 8).

The most represented patient groups were those with the luminal A and luminal B ($HER2^-$) molecular subtypes. Patients with $HER2^+$ [including luminal B ($HER2^+$)] subtypes accounted for only 3 and 2 cases, respectively, and were therefore excluded from the analysis due to small sample sizes (Figure 9). It was observed that patients with the luminal B ($HER2^-$) subtype had a higher proportion of CD163-positive hybrid cells.

The median proportion of $CD68^-CD163^+CD16^-CD206^-CD45^+EpCAM^+panCK^+$ cells was 0.00% (0.00–0.00) in patients with the luminal A subtype, whereas it increased to 0.80% (0.00–15.40%) in patients with the luminal B ($HER2^-$) subtype ($p = 0.0495$). $CD68^+CD163^+CD16^-CD206^+$ $CD45^+EpCAM^+panCK^+$ cells have median proportions of 0.00% (0.00–5.83%) in luminal A and 15.80% (1.50–36.40%) in luminal B ($HER2^-$) patients, respectively ($p = 0.0212$).

Within the $CD45^+EpCAM^+panCK^-$ hybrid cells, a subpopulation with a significantly higher proportion in luminal B ($HER2^-$) patients was also identified ($p = 0.0481$) (Figure 9). The median proportion of $CD68^-CD163^+CD16^-CD206^+$ cells among this group was 16.70% (0.00–33.30%) in luminal A and 40.00% (0.00–66.70%) in luminal B ($HER2^-$), respectively.

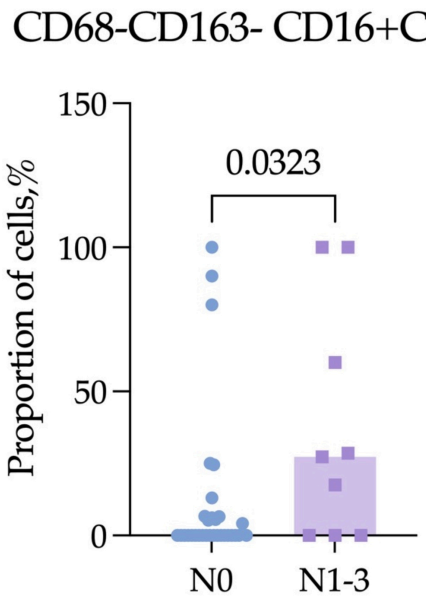


Figure 8. Proportion of CD68$^-$CD163$^-$CD16$^+$CD206$^-$ cells among CD45$^+$EpCAM$^+$panCK$^+$ tumor-immune hybrid cells in patients stratified by the N parameter, *n* = 42.

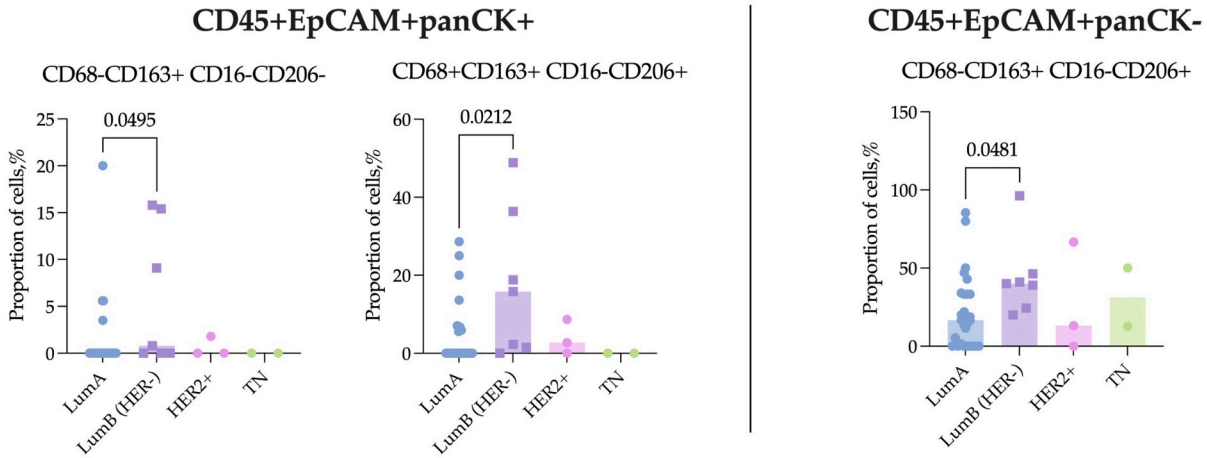


Figure 9. Expression patterns of macrophage/monocyte markers CD68, CD163, CD16, and CD206 in patients stratified by the molecular subtype, *n* = 42.

Comparison of the proportions of different hybrid cell subpopulations in relation to tumor invasion and tumor grade revealed no significant differences between patient groups ($p > 0.05$); data were not shown.

Hybrid cells as potential prognostic markers of tumor progression during patient follow-up

During the 3-year follow-up period, distant organ metastases developed in 4 of 42 patients, including 2 cases of bone metastases and one case each of lung and ovarian metastases. Comparison of the hybrid cell subpopulation composition between patients with and without distant metastases during follow-up revealed significant differences across the three studied subpopulations (Figure 10). All identified subpopulations exhibited increased proportions of cells in patients who experienced progression during the follow-up period; significance levels are detailed in Figure 10A–C (medians and interquartile ranges are provided).

To evaluate the prognostic significance for all detected populations, ROC analysis was performed. Only two of the six populations (CD68$^+$CD163$^+$CD16$^-$CD206$^-$CD45$^+$EpCAM$^-$panCK$^+$ and CD68$^-$CD163$^-$CD16$^-$CD206$^+$CD45$^+$EpCAM$^+$panCK$^+$ hybrid cells) were predicted outcome (Figure 11A).

The proportion of CD45$^+$EpCAM$^-$panCK$^+$CD68$^+$CD163$^+$CD16$^-$CD206$^-$ cells exceeding 0.65% predicted distant metastases within a 3-year follow-up period, with 97.30% specificity and 75.00% sensitivity [area

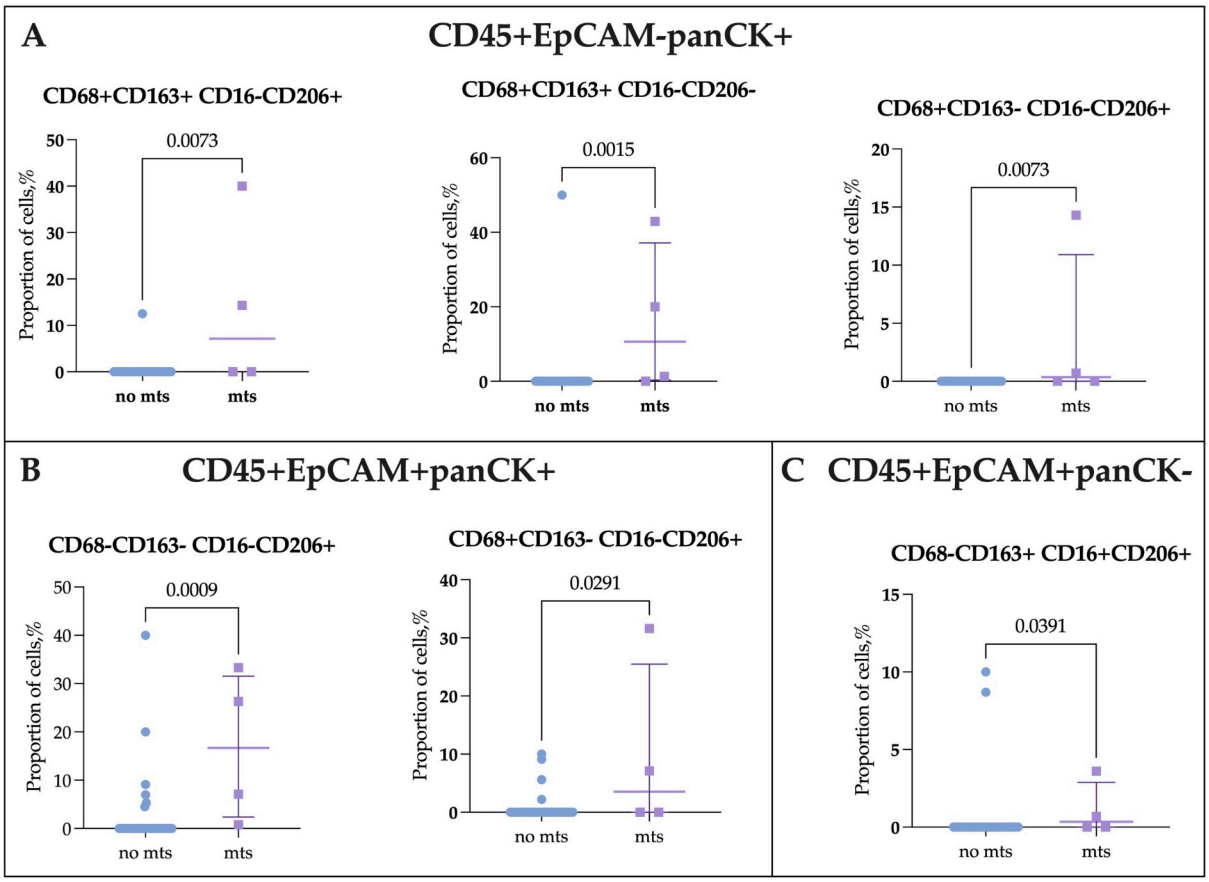


Figure 10. Comparison of tumor-immune hybrid cell subpopulation composition in breast cancer patients with ("mts", *n* = 4) and without distant metastasis ("no mts", *n* = 38) during the follow-up period.

under the curve (AUC) = 0.8514, $p = 0.0223$], yielding a diagnostic accuracy of 95.65%. The median survival time for patients with the proportion of the indicated cells above the established cut-off was 22.5 months, whereas the median survival time for the group with proportions below the cut-off was 7.5 months.

Similarly, the proportion of $CD45^+EpCAM^+panCK^+CD68^-CD163^-CD16^-CD206^+$ THCs above 0.40% predicted distant metastasis during follow-up with 84.21% specificity and 100.00% sensitivity (AUC = 0.9276, $p = 0.0054$), and a diagnostic accuracy of 85.71%. The median survival time for patients with the proportion of the indicated cells above the established cut-off was 19.0 months, whereas the median survival time for the group with proportions below the cut-off was 5.5 months.

Patients exhibiting proportions of $CD68^+CD163^+CD16^-CD206^-$ and $CD68^-CD163^-CD16^-CD206^+$ cells above these thresholds demonstrated significantly lower distant metastasis free survival (DMFS) compared to those below the thresholds ($p = 0.012$ and $p = 0.0223$, respectively) (Figure 11B) (Table 2).

Table 2. Tumor-immune hybrid cell phenotypes with potential prognostic significance.

THC phenotypes	Cut-off value	AUC	Sensitivity	Specificity	*P*-value
$CD45^+EpCAM^-panCK^+CD68^+CD163^+CD16^-CD206^-$	0.65%	0.8514	75.00%	97.30%	0.0223
$CD45^+EpCAM^+panCK^+CD68^-CD163^-CD16^-CD206^+$	0.40%	0.9276	100.00%	84.21%	0.0054

Discussion

In this study, we analyzed phenotypic variants of THCs co-expressing pan-leukocyte marker CD45 and epithelial markers EpCAM and/or pan-cytokeratin in primary breast tumors. The data demonstrate that the hybrid cell population is heterogeneous and contains phenotypic variants associated with clinicopathological features and disease prognosis.

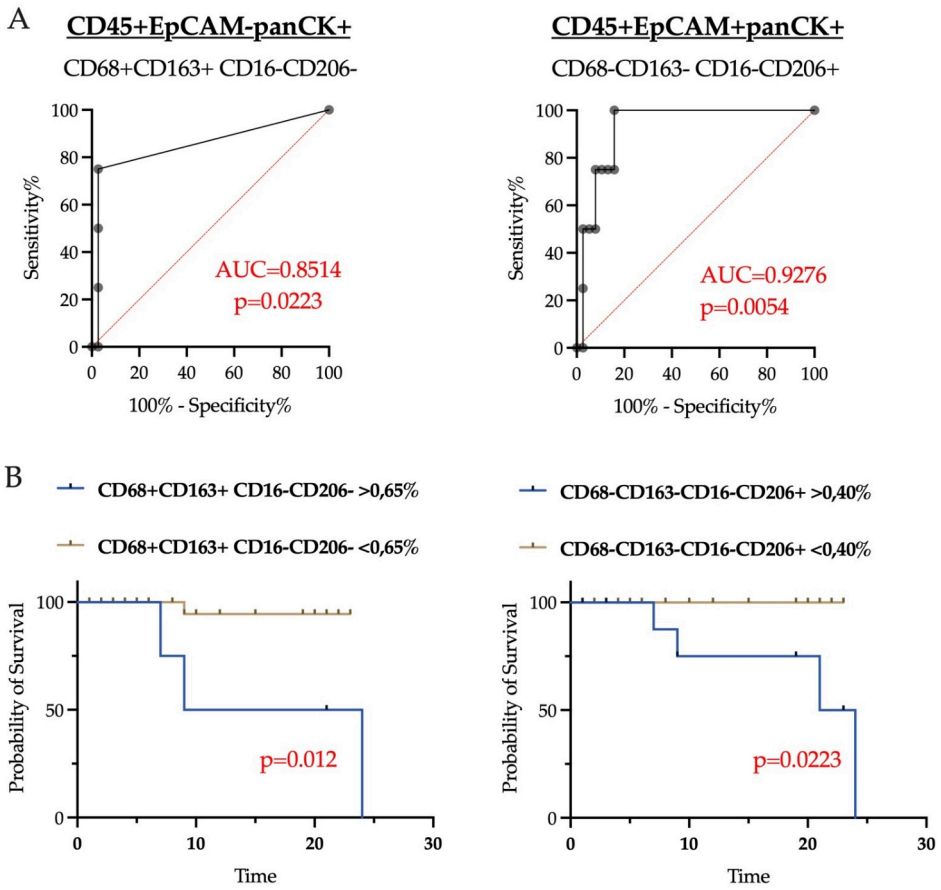


Figure 11. ROC analysis of CD68$^+$CD163$^+$CD16$^-$CD206$^-$ (among CD45$^+$EpCAM$^-$panCK$^+$) and CD68$^-$CD163$^-$CD16$^-$CD206$^+$ (among CD45$^+$EpCAM$^+$panCK$^+$) hybrid cells (A) and distant metastasis-free survival in breast cancer patients stratified by cell proportions (B).

In primary breast tumors, THCs expressing EpCAM (CD45$^+$EpCAM$^+$panCK$^-$ and CD45+EpCAM$^+$panCK$^+$) were most frequently detected, whereas cells expressing only pan-cytokeratin (CD45$^+$EpCAM$^-$panCK$^+$) were found significantly less often and in smaller quantities. Our previous study also noted the lowest proportion of hybrid cells with monoexpression of cytokeratins in an independent BC patient cohort [17]. Notably, in the current study, the EpCAM$^-$panCK$^+$ epithelial phenotype predominated within the total tumor cell population. EpCAM serves as an adhesion molecule involved in proliferation and migration, and it likely plays a key role in cell fusion with leukocyte-origin cells [18]. The presence of EpCAM likely facilitates cell-cell interactions essential for hybrid formation, whereas its absence, despite its prevalence in the tumor, is associated with a diminished capacity of tumor cells to fuse with CD45$^+$ cells.

Detailed analysis of macrophage/monocyte marker expression (CD68, CD163, CD16, CD206) revealed significant differences between THCs subpopulations. EpCAM$^+$ THCs (CD45$^+$EpCAM$^+$panCK$^-$ and CD45$^+$EpCAM$^+$panCK$^+$) exhibited a significant proportion of subpopulations expressing M2 polarization markers (CD163 and CD206), suggesting their potential immunosuppressive and pro-tumor role [19]. Experimental evidence supports a higher capacity of M2-polarized monocytes versus M1 to fuse with tumor cell lines, forming invasive tumor-hybrid cells [9]. The predominance of M2-like (CD163$^+$, CD206$^+$) hybrid subpopulations among EpCAM$^+$ tumor cells aligns with the established role of TAMs in promoting immunosuppression, angiogenesis, and metastasis [20]. Conversely, the least represented CD45$^+$EpCAM$^-$panCK$^+$ subpopulation predominantly lacked expression of these macrophage/monocyte markers, indicating that these hybrids may arise preferentially from fusion with CD45$^+$ cells of non-macrophage/monocyte origin to a greater extent than the other hybrid subpopulations. In any case, hybridization of tumor cells with immune-origin cells (whether macrophages or others) may enable the hybrids to acquire advantageous traits from both cell types. Specifically, they may combine the invasive and mutational characteristics of cancer cells with the mobility and immune evasion capabilities of immune cells. This combination potentially drives metastasis, treatment resistance, and immune evasion [9].

The identified associations between THC phenotypes and clinicopathological features underscore their potential clinical significance. An increased proportion of THCs expressing macrophage markers CD163 and/or CD16 in larger tumors (stage T2) and in cases with lymph node metastases (N1–3) suggests that hybridization between tumor cells and macrophage/monocyte-lineage cells is linked to disease aggressiveness. Notably, subpopulations detected in patients at stage T2 exhibited both presence and absence of the macrophage marker CD68. This phenomenon may reflect early macrophage differentiation from circulating monocytes, during which CD68 may be insufficiently expressed for detection [21]. Furthermore, the observed increase in $CD16^+$ THCs lacking CD68, CD163, and CD206 in patients predominantly with N1–3 lymph node involvement may suggest possible hybrid formation with NK cells, which express CD16 but lack indicated macrophage polarization markers. This aspect constitutes a limitation of the study; to clarify the nature of this hybrid cell subpopulation, assessment of CD56 expression is warranted, as CD56 can discriminate NK cells from macrophages.

Of particular interest are the detected differences in the composition of the THC population associated with BC molecular subtypes. In patients with the luminal B ($HER2^-$) subtype—which is known to have a more aggressive clinical course compared to luminal A [22]—a significant increase in the proportion of hybrids expressing M2 macrophage markers CD163 and CD206 was observed. M2 macrophages, unlike M1, have been shown to promote tumor cell proliferation both in vitro and in vivo [23, 24]. Given that luminal A and luminal B ($HER2^-$) differ primarily in the Ki-67 proliferation index, it is plausible to speculate that hybrid cells with an M2-like phenotype contribute to the mechanisms underlying the more unfavorable clinical outcome of the luminal B ($HER2^-$) subtype.

The most promising finding of this study, which warrants validation in a larger cohort, is the identification of THC populations associated with distant metastasis during a 3-year follow-up. High prognostic accuracy was observed for the $CD68^+CD163^+CD16^-CD206^-$ phenotype within the $CD45^+EpCAM^-panCK^+$ subpopulation, and the $CD68^-CD163^-CD16^-CD206^+$ phenotype within the $CD45^+EpCAM^+panCK^+$ subpopulation, suggesting these phenotypes could serve as potential predictors of BC progression. Importantly, the most prevalent $CD45^+EpCAM^+panCK^-$ hybrid tumor cell subset did not correlate with clinical prognosis. Notably, the minor $CD45^+EpCAM^-panCK^+$ fraction expressing both CD68 and CD163 exhibited the highest diagnostic accuracy (95.65%). Although these cells were present at very low levels (cutoff 0.65%), their presence was significantly associated with worse distant metastasis-free survival ($p = 0.012$). In the context of the M1/M2 paradigm, which represents the extremes of a functional continuum rather than rigid cell types, we can suppose that the existence of such unconventional cell phenotypes (the expression of CD163 in the absence of CD206 expression) may be explained by the high plasticity of macrophages in the expression of polarization markers [25]. This is confirmed by observations of other authors. Fang et al. [26] showed that TAMs in BC, characterized by isolated expression of CD163 and CD206, localize to different tumor regions. $CD163^+$ TAMs are found in both stromal and tumor compartments and tend to infiltrate the tumor nest, whereas $CD206^+$ TAMs are predominantly located in the stroma [26]. The absence of $CD206^+$ TAMs within the tumor body in BC has also been previously reported [27]. Furthermore, similar spatial distribution of these two TAM subsets has been demonstrated in gastric cancers [28]. These observations suggest that CD163 and CD206 identify distinct TAM subsets. Thus, biologically, the subpopulation identified in our study may exhibit an M2-like macrophage phenotype characterized by the expression of CD68 and CD163 and potentially originate from the tumor nest.

However, our study has several important limitations to consider when interpreting the results. The relatively small sample size (42 patients) and the limited number of progression cases (4 patients) necessitate validation of these findings in larger, independent cohorts and can be clarified through further longitudinal observation. Thus, the data obtained are preliminary and require an increased sample size and longer follow-up period. Additionally, although flow cytometry offers higher throughput and sensitivity, particularly for detecting rare cell populations, complementary immunohistochemistry analyses of hybrid cells would have provided valuable spatial and morphological context to enhance the data interpretation.

Conclusion

The data obtained indicate that THCs within the primary breast tumor constitute a heterogeneous population. Expression of EpCAM appears to be associated with more efficient hybrid formation with $CD45^+$ cells in the TME. Hybrid cells exhibiting an M2-like phenotype, characterized by expression of CD163 and CD206, are correlated with more advanced T and N stages.

Moreover, hybrid cells with the phenotypes $CD68^+CD163^+CD16^-CD206^-$ (within the $CD45^+EpCAM^-panCK^+$ subpopulation) and $CD68^-CD163^-CD16^-CD206^+$ (within the $CD45^+EpCAM^+panCK^+$ subpopulation), after appropriate validation, may serve as potential prognostic markers for distant metastasis development and reduced distant metastasis-free survival. These phenotypes hold potential as therapeutic targets and as biomarkers for stratifying patients at high risk of disease progression.

Abbreviations

AUC: area under the curve

BC: breast cancer

CD45: cluster of differentiation 45

DMFS: distant metastasis free survival

EpCAM: epithelial cell adhesion molecule

HER2: human epidermal growth factor receptor 2

NK: natural killer

ROC: receiver operating characteristic

TAMs: tumor-associated macrophages

THCs: tumor-immune hybrid cells

TME: tumor microenvironment

Supplementary materials

The supplementary figure for this article is available at: https://www.explorationpub.com/uploads/Article/file/1002411_sup_1.pdf.

Declarations

Acknowledgments

The authors thank the Core Facility “Medical Genomics” at Tomsk National Research Medical Center (Tomsk NRMC) for providing access to the equipment used in this study.

Author contributions

ESG: Conceptualization, Investigation, Formal analysis, Visualization, Writing—original draft, Writing—review & editing. AYK, EOS, EVK: Investigation, Validation, LAT: Writing—review & editing, Supervision. All authors read and approved the submitted version.

Conflicts of interest

The authors declare that they have no conflicts of interest related to this work.

Ethical approval

The study received approval from the local ethics committee of the Tomsk NRMC Institutional Review Board on August 25, 2020, with approval No. 7.

Consent to participate

Informed consent to participate in the study was obtained from all participants.

Consent to publication

Informed consent to publication was obtained from relevant participants.

Availability of data and materials

The datasets supporting the findings of this study are available from the corresponding author upon reasonable request.

Funding

The authors received no financial support for the research, authorship, and/or publication of this article.

Copyright

© The Author(s) 2026.

Publisher's note

Open Exploration maintains a neutral stance on jurisdictional claims in published institutional affiliations and maps. All opinions expressed in this article are the personal views of the author(s) and do not represent the stance of the editorial team or the publisher.

References

1. Krystel-Whittemore M, Tan PH, Wen HY. Predictive and prognostic biomarkers in breast tumours. Pathology. 2024;56:186–91. [DOI] [PubMed] [PMC]
2. Tian Y, Yang Y, He L, Yu X, Zhou H, Wang J. Exploring the tumor microenvironment of breast cancer to develop a prognostic model and predict immunotherapy responses. Sci Rep. 2025;15:12569. [DOI] [PubMed] [PMC]
3. Liu K, Shi J, Liu J, Zhang Y, Liang J, Xu J, et al. The influence of cell-cell fusion on cancer heterogeneity and its promise for targeted treatments. Cell Oncol (Dordr). 2026;49:22. [DOI] [PubMed] [PMC]
4. Cozzo AJ, Coleman MF, Hursting SD. You complete me: tumor cell-myeloid cell nuclear fusion as a facilitator of organ-specific metastasis. Front Oncol. 2023;13:1191332. [DOI] [PubMed] [PMC]
5. Zucker A, Anderson AN, Ekstrom TJ, Fowler KL, Giske NR, Moore AG, et al. Tumor-immune hybrid cell biology: A review of its potential impact in oncology. Cancer Lett. 2026;641:218313. [DOI] [PubMed]
6. Hass R, von der Ohe J, Dittmar T. Hybrid Formation and Fusion of Cancer Cells In Vitro and In Vivo. Cancers. 2021;13:4496. [DOI] [PubMed] [PMC]
7. Xiao M, Li X. The impact of the tumor microenvironment on macrophages. Front Immunol. 2025;16:1572764. [DOI] [PubMed] [PMC]
8. Wei G, Li B, Huang M, Lv M, Liang Z, Zhu C, et al. Polarization of Tumor Cells and Tumor-Associated Macrophages: Molecular Mechanisms and Therapeutic Targets. MedComm. 2025;6:e70372. [DOI] [PubMed] [PMC]
9. Aguirre LA, Montalbán-Hernández K, Avendaño-Ortiz J, Marín E, Lozano R, Toledano V, et al. Tumor stem cells fuse with monocytes to form highly invasive tumor-hybrid cells. OncoImmunology. 2020;9:1773204. [DOI] [PubMed] [PMC]
10. Strizova Z, Benesova I, Bartolini R, Novysedlak R, Cecrdlova E, Foley LK, et al. M1/M2 macrophages and their overlaps – myth or reality? Clin Sci (Lond). 2023;137:1067–93. [DOI] [PubMed] [PMC]
11. Akhter MZ, Sharawat SK, Kumar V, Kochat V, Equbal Z, Ramakrishnan M, et al. Aggressive serous epithelial ovarian cancer is potentially propagated by EpCAM+CD45+ phenotype. Oncogene. 2018;37:2089–103. [DOI] [PubMed]

12. Lu S, Sun Z, Liu L, Li P, Li B, Li W, et al. Tumor-Derived Exosomes Regulate Apoptosis of CD45+ EpCAM+ Cells in Lung Cancer. Front Immunol. 2022;13:903882. [DOI] [PubMed] [PMC]
13. Mousset CM, Hobo W, Woestenenk R, Preijers F, Dolstra H, van der Waart AB. Comprehensive Phenotyping of T Cells Using Flow Cytometry. Cytometry A. 2019;95:647–54. [DOI] [PubMed]
14. Loibl S, André F, Bachelot T, Barrios CH, Bergh J, Burstein HJ, et al.; ESMO Guidelines Committee. Electronic address: clinicalguidelines@esmo.org. Early breast cancer: ESMO Clinical Practice Guideline for diagnosis, treatment and follow-up. Ann Oncol. 2024;35:159–82. [DOI] [PubMed]
15. Xu Y, Wang X, Liu L, Wang J, Wu J, Sun C. Role of macrophages in tumor progression and therapy (Review). Int J Oncol. 2022;60:57. [DOI] [PubMed] [PMC]
16. Bied M, Ho WW, Ginhoux F, Blériot C. Roles of macrophages in tumor development: a spatiotemporal perspective. Cell Mol Immunol. 2023;20:983–92. [DOI] [PubMed] [PMC]
17. Mukhamedzhanov RK, Grigoryeva ES, Tashyreva LA, Perelmuter VM, Zavyalova MV, Savelieva OE. Assessment of metastatic traits of the cells with hybrid phenotype in breast cancer. Bulletin of RSMU. 2023:4–15. [DOI]
18. Huang L, Yang Y, Yang F, Liu S, Zhu Z, Lei Z, et al. Functions of EpCAM in physiological processes and diseases (Review). Int J Mol Med. 2018;42:1771–85. [DOI] [PubMed] [PMC]
19. Wang S, Wang J, Chen Z, Luo J, Guo W, Sun L, et al. Targeting M2-like tumor-associated macrophages is a potential therapeutic approach to overcome antitumor drug resistance. npj Precis Oncol. 2024;8:31. [DOI] [PubMed] [PMC]
20. Jayasingam SD, Citartan M, Thang TH, Mat Zin AA, Ang KC, Ch'ng ES. Evaluating the Polarization of Tumor-Associated Macrophages Into M1 and M2 Phenotypes in Human Cancer Tissue: Technicalities and Challenges in Routine Clinical Practice. Front Oncol. 2020;9:1512. [DOI] [PubMed] [PMC]
21. Furgiuele S, Descamps G, Cascarano L, Boucq A, Dubois C, Journe F, et al. Dealing with Macrophage Plasticity to Address Therapeutic Challenges in Head and Neck Cancers. Int J Mol Sci. 2022;23:6385. [DOI] [PubMed] [PMC]
22. Inic Z, Zegarac M, Inic M, Markovic I, Kozomara Z, Djurisic I, et al. Difference between Luminal A and Luminal B Subtypes According to Ki-67, Tumor Size, and Progesterone Receptor Negativity Providing Prognostic Information. Clin Med Insights: Oncol. 2014;8:107–11. [DOI] [PubMed] [PMC]
23. Zhang C, Wei S, Dai S, Li X, Wang H, Zhang H, et al. The NR_109/FUBP1/c-Myc axis regulates TAM polarization and remodels the tumor microenvironment to promote cancer development. J ImmunoTher Cancer. 2023;11:e006230. [DOI] [PubMed] [PMC]
24. Munir MT, Kay MK, Kang MH, Rahman MM, Al-Harrasi A, Choudhury M, et al. Tumor-Associated Macrophages as Multifaceted Regulators of Breast Tumor Growth. Int J Mol Sci. 2021;22:6526. [DOI] [PubMed] [PMC]
25. Vitale I, Manic G, Coussens LM, Kroemer G, Galluzzi L. Macrophages and Metabolism in the Tumor Microenvironment. Cell Metab. 2019;30:36–50. [DOI] [PubMed]
26. Fang C, Cheung MY, Chan RC, Poon IK, Lee C, To CC, et al. Prognostic Significance of CD163+ and/or CD206+ Tumor-Associated Macrophages Is Linked to Their Spatial Distribution and Tumor-Infiltrating Lymphocytes in Breast Cancer. Cancers. 2024;16:2147. [DOI] [PubMed] [PMC]
27. Egeblad M, Ewald AJ, Askautrud HA, Truitt ML, Welm BE, Bainbridge E, et al. Visualizing stromal cell dynamics in different tumor microenvironments by spinning disk confocal microscopy. Dis Model Mech. 2008;1:155–67. [DOI] [PubMed] [PMC]
28. Huang YK, Wang M, Sun Y, Di Costanzo N, Mitchell C, Achuthan A, et al. Macrophage spatial heterogeneity in gastric cancer defined by multiplex immunohistochemistry. Nat Commun. 2019;10:3928. [DOI] [PubMed] [PMC]